Identifying nano-Schottky diode currents in silicon diodes with 2D interfacial layers

Tihomir Knežević[1], Lis K. Nanver[2],

[1] *Ruđer Bošković Institute*, Zagreb, Croatia

[2] *MESA+ Institute of Nanotechnology*, *University of Twente*, Enschede, The Netherlands

2023 35th International Conference on Microelectronic Test Structure (ICMTS) | 979-8-3503-4653-4/23/$31.00 ©2023 IEEE | DOI: 10.1109/ICMTS55420.2023.10094164

***Abstract*—In silicon technology, Schottky diodes mainly exhibit high current levels, and attempts are regularly made to reduce these by introducing 2D layers between the metal contact and the silicon. Defects in such interfacial layers, from weakly bonded structures to actual pinholes, can lead to high, localized metal-semiconductor Schottky currents. Using the example of diodes with an interfacial layer of pure boron (PureB) between an aluminum metallization layer and the Si, a signature for such "nano-Schottky's" is determined by evaluating the results of several different test-structure arrays and measurement techniques. An adapted bipolar-type measurement is introduced as an additional method to determine whether any high current characteristics originate from a low Schottky barrier height over the entire diode surface or from a localized nano-Schottky structure.**

Keywords—diode characterization, pure boron, nano-Schottky, 2D interfacial layers, bipolar devices

I. Introduction

This paper first reviews a series of studies in which nano-Schottky diodes have been recognized as the source of undesirably high leakage currents in silicon diodes with otherwise low saturation current, fabricated with a nm-thin pure boron layer deposited between metal and silicon. This so-called PureB technology has been particularly successful in the development and commercialization of silicon photodiode detectors for low-penetration-depth beams, which are now used in deep-ultraviolet (DUV)/extreme-ultraviolet (EUV) lithography systems [1, 2] and low-energy-electron scanning-electron-microscopy (SEM) systems [3, 4].

Today, other 2D interfacial layers are often studied in both Si and III-V diodes to lower the leakage current by modifying the barrier height and/or reducing the interface states. In diode applications, there is usually a tradeoff between layer thickness and series resistance. When using insulating materials, this requires a tunneling layer thickness or low breakdown voltage across the insulator [5, 6]. In compound semiconductor transistors, extensive research is underway to develop metal-insulator-semiconductor (MIS) gates with dielectrics such as Al_2O_3 and SiN_x [7] to replace the commonly used Schottky gate diodes. When the basic diode characteristics are preserved, these gates are referred to as MIS Schottky diodes. Otherwise, in the case of a gate capacitor, the use of the thinnest possible insulator is still aspired if a high capacitive coupling to the channel is to be maintained [8, 9]. In all cases, localized nano-Schottky's, formed at weak spots where the metal inadvertently either comes close to or even touches the semiconductor can be the source of excessively high currents.

In many cases, material traps, particularly at the interface, can also significantly increase the leakage current, which can obscure the existence of localized nano-Schottky's. The PureB devices, that we discuss here, exhibit a high degree of perfection that has allowed us to determine the signature of nano-Schottky's in the diode *I-V* characteristics. The conclusions are based on statistical data, measurement of arrays of diodes with varying geometry, and temperature-dependent characteristics. In addition, a special bipolar-type measurement using the 2-diode method [10, 11] is described and evaluated as an aid in identifying nano-Schottky behavior. Specific 2-diode test structures that can be used as a means to confirm the localized nature of a nano-Schottky are also discussed.

II. Test Methods

A. Statistical I-V Characterization

The identification of a low distribution of nano-Schottky's on the diode area can be facilitated by statistical measurement of a large number of diodes. This was illustrated in [12], where advantage was taken of the fact that the 2D boron layer itself creates the p^+-type region of the p^+n-like diodes under investigation [13]. This gave us the possibility to remove the metal on parts of the diode surface, as illustrated in Fig. 1. For the PureB devices in this study, a few nm thick B deposition was performed by chemical-vapor deposition at 700°C as described in [1]. This creates a high concentration of fixed negative charge at the interface that attracts a hole layer, forming a p-region with a high effective Gummel number to efficiently suppress electron injection. The metallurgic junction is then only a few nm away from Al metallization, but the B layer is an efficient material barrier between the Si and Al. If the Si surface has some (particle) contamination that prevents B adsorption during deposition, weak spots and pinholes can result in local Al contacting of the Si.

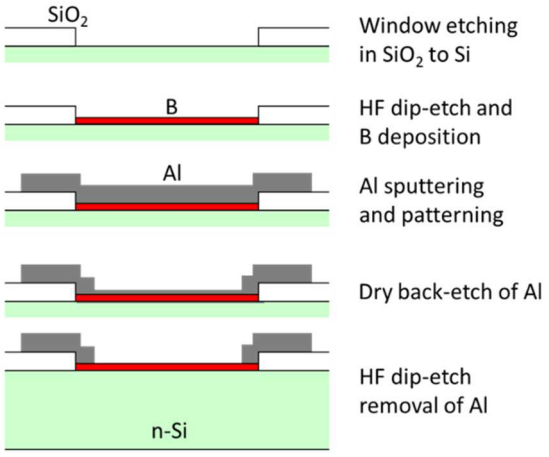

Fig. 1. Basic PureB Si diode process flow using Al as anode metal. In the last 2 steps, the Al is removed in the diode center for application as a photodiode.

The test structure used was an array of 300×300 μm^2 diodes with different metal coverage of the diode perimeter, as shown in Fig. 2a. The n-substrate resistivity is 2-5 Ω-cm. An example of the *I-V* characteristics measured across several arrays is shown in Fig. 2b for sets with a 12 nm thick B-layer and in Fig. 2c for a much thinner 4 nm one. For the former, all currents were low and ideal. With the thin B-layer, high currents were observed at a frequency that correlated to the amount of metal coverage. In Fig. 2d the distribution of currents at 0.2 V forward voltage is plotted, firmly establishing the statistical relationship between the high currents and the amount of metal coverage. At higher voltages above about 0.5 V forward bias, the higher currents return to the ideally low p$^+$n-junction values, resulting in a kink in the forward characteristic. Both regions of the *I-V* curve have an ideality factor n = 1, indicating that the high current is related to diode behavior and not to a short circuit.

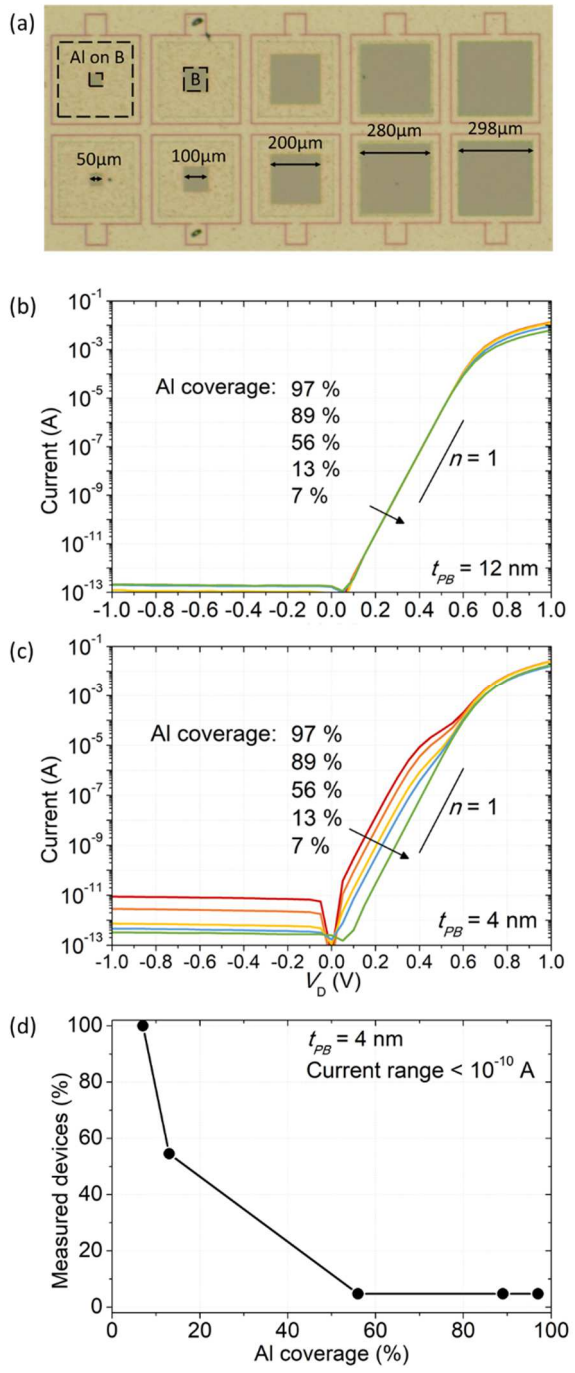

Fig. 2: (a) Micro-image of 300×300 μm^2 diodes in a test structure array with different metal coverage of the diode perimeters. Measured *I-V* characteristics of an array with a B-layer thickness, t_{PB}, of (b) 12 nm and (c) 4 nm. The distance between 2 adjacent diodes is 96 μm. (d) Distribution of devices with currents less than 10^{-10} A at a forward voltage of 0.2 V [12].

In all the examples discussed in the following, it was validated that the source of abnormally high current levels was due to the presence of very small Schottky-like diodes that we will refer to as nano-Schottky diodes. When the total nano-Schottky current and/or diode series resistance was high enough, the diode current was attenuated before the kink appeared. The devices discussed in Section II.C are an example of this. Otherwise, the high excess currents were about a decade or so higher than the ideal p$^+$n currents and the kinked behavior was evident. We believe that it is caused by high-injection effects at the nano-Schottky junction [12, 14].

B. Temperature Dependent I-V Characterization

A clear confirmation that the currents perceived to originate from nano-Schottky's actually exhibit Schottky-like behavior was provided by the temperature-dependent measurements discussed in detail in [14]. An example of two 300×300 μm^2 diodes, both of which appeared to be ideal at 373 K, is shown in Fig. 3. As the temperature is lowered to 223 K, a distinct kink appears in the diode with the largest metal coverage. Once the kink is clearly discerned, the ideality factor in the low voltage, high current region was n = 1. In the intermittent temperature region, extraction of n yielded values above 1, which could be mistaken for trap-induced leakage current. All-in-all, such temperature-dependent characterization is an ideal tool for identifying the origin of non-ideal *I-V* currents, but the measurements can be tedious and have relatively low availability.

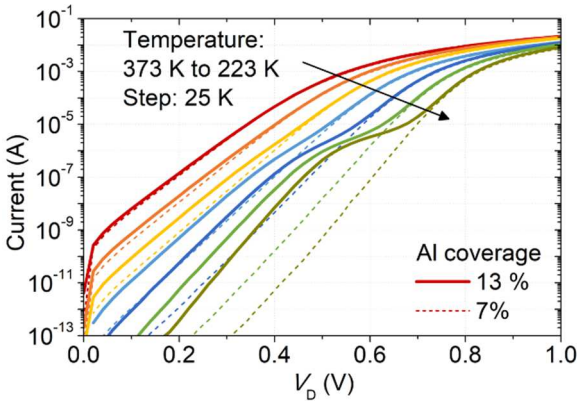

Fig. 3. Temperature-dependent measured *I–V* characteristics of two 300×300 μm^2 PureB diodes with t_{PB} = 4 nm, one with 7% metal coverage showing ideal behavior down to 223 K, and the other with 13% coverage displaying visible kinked behavior only as the temperature is lowered [14].

C. Nano-Schottky's related to Perimeter Defects

The design of large photodiodes with p$^+$n junction anodes mainly includes the use of guard rings to mitigate high electric fields often associated with the strong curvature of diffused regions at the diode perimeter. Such high electric fields also occur at the perimeter of PureB diodes [15]. In addition, these diodes can also be degraded by imperfect B coverage of the Si at the perimeter. Weak spots where metal is more likely to seep through to the Si are therefore more frequently found at the diode edges.

In small diodes, it can be more economical to apply an implicit guard ring, such as the phosphorus implanted regions used in the single photon avalanche diodes (SPADs) described

in [4]. Thus, the Si at the perimeter of these PureB diodes was only separated from the Al metal by the B-layer. In one series of such photodiodes, abnormally high currents were identified as nano-Schottky's formed at the perimeter. This was established by measuring arrays of devices with different metal coverage and area/perimeter ratios. Examples of measurements are shown in Fig. 4 [16]. In addition, light emission from diodes under forward bias as well as reverse bias avalanching was used as a diagnostic tool to identify the location of other types of defects, which further confirmed the conclusions regarding nano-Schottky's at the perimeter.

D. 2-Diode Differential Current Extraction

In the present paper, we investigate whether the 2-diode measurement technique using differential current extraction can be useful for confirming the presence of nano-Schottky's. In the past, this method was used to obtain information on the ratio between the diode hole-to-electron currents in order to identify the dominant carrier type. The basic measurement method is illustrated in Fig. 5. The current through two adjacent diodes is measured in two different biasing modes and the differential current is extracted. Fig. 5b depicts a standard bipolar junction transistor (BJT) Gummel plot measurement with the diode under test (DUT) as the emitter, the adjacent diode as the collector, and the substrate as the base. The first mode of the 2-diode technique, shown in Fig. 5c is to measure the emitter current, I_E, as a function of forward bias voltage. The second mode, shown in Fig. 5d, is to measure the emitter current, $I_{E//C}$, with the emitter and collector following the same forward voltage sweep. The resulting differential current $\Delta I_E = I_E - I_{E//C}$, was found in [10]

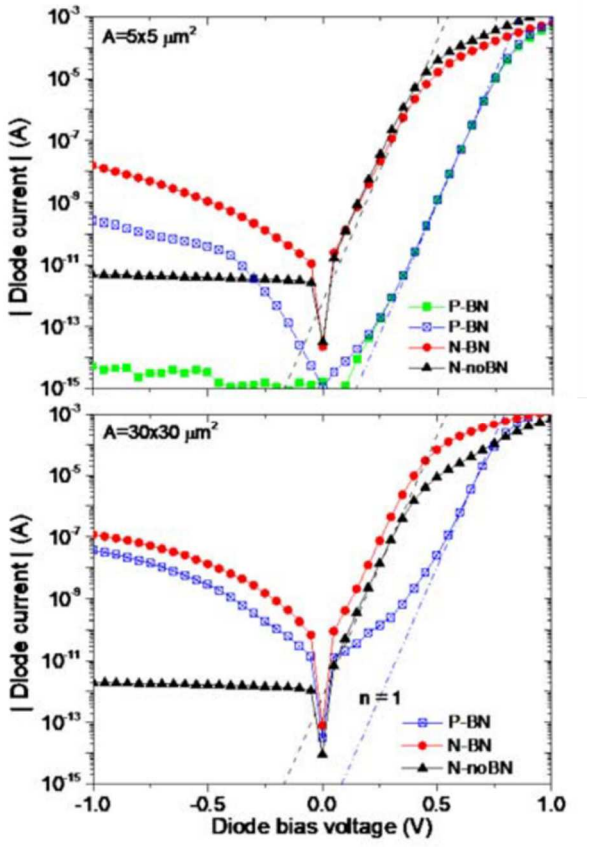

Fig. 4. Examples of PureB photodiode *I-V* characteristics measured in [16], with diode areas 5×5 μm² and 30×30 μm². Poor B coverage at the diode perimeter resulted in a high frequency of nano-Schottky formation in the N-BN and N-noBN devices.

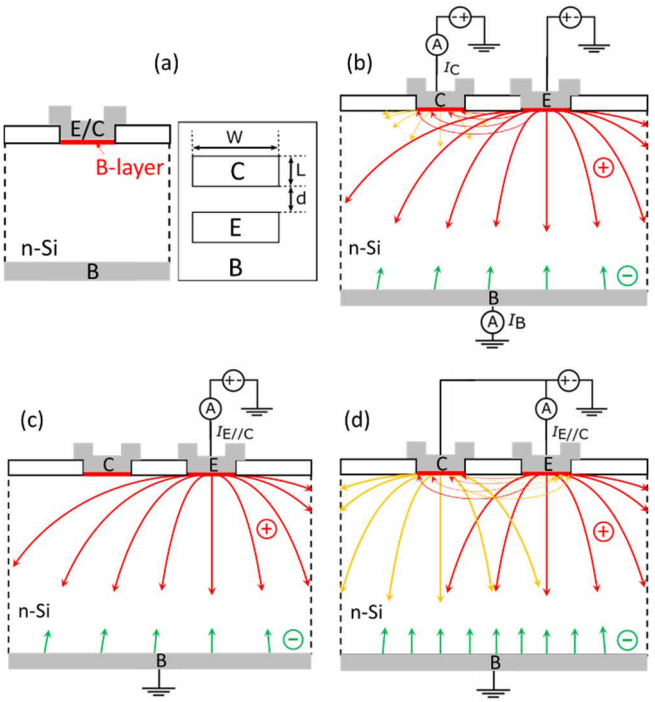

Fig. 5. (a) Schematic cross-section and layout of the 2-diode test structures. (b) BJT biasing for measuring I_C. Biasing for (c) the single diode measurement of I_E, and (d) the 2-diode measurement of $I_{E//C}$. The expected current flows are indicated by green and red/orange arrows for the electron and hole currents, respectively. The arrow length indicates the relative magnitude of the currents for the case where the electron current flows are much smaller than the hole currents.

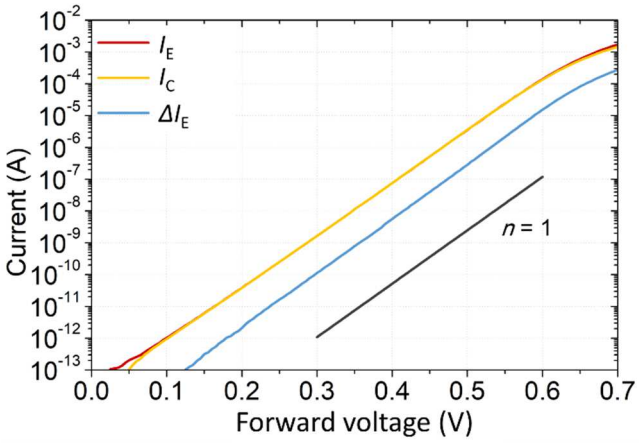

Fig. 6. *I-V* characteristics of two adjacent 300×300 μm² diodes and the extracted differential current ΔI_E.

to be related to the difference in hole current spreading into the substrate.

The 2-diode technique proved to be useful when the electron current is smaller or not much larger than the hole current. It was shown that any leakage current from generation-recombination (*g-r)* centers in the vicinity of the p^+ regions was eliminated in the differential current ΔI_E that hence displayed an $n = 1$. Such cases are treated in detail in [10]. Here we study the diodes discussed in Section II.A, many of which were ideal. An example of the 2-diode extraction of ΔI_E for an ideal pair is shown in Fig. 6. All *I-V* curves have $n = 1$ until attenuation from the series resistance becomes apparent above 0.55 V forward voltage.

As opposed to the ideal low-electron-current case, if the electron current became decades higher than the hole current, the level and ideality of ΔI_E were affected [10, 11]. An example with Schottky diode emitter and collector is shown in Fig. 7. The electron current is more than 4 decades higher than the hole current. The ΔI_E behaves in a manner typical of such a high electron-to-hole ratio when both I_E and $I_{E//C}$ are measurably attenuated by substrate resistance over the whole forward bias region. The ΔI_E characteristic displays 3 basic regions: (i) the highest current region with n > 1; (ii) the medium-high current region with n less than 1 and decreasing with decreasing bias voltage; and (iii) the low current region where ΔI_E becomes negative, i.e., $I_{E//C}$ becomes higher than I_E.

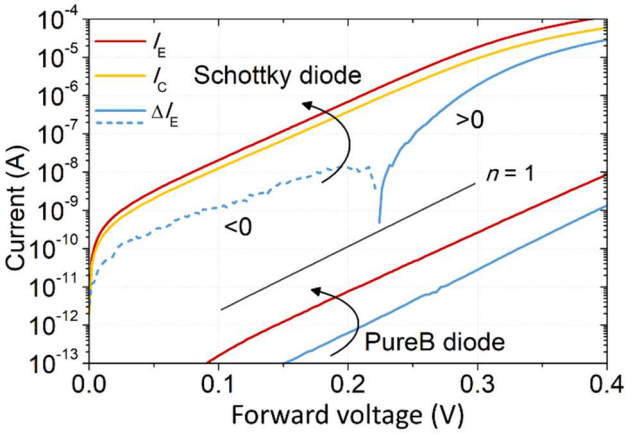

Fig. 7. The 2-diode *I-V* characteristics of a pair of Al-Si Schottky diodes with an area of 40×1 μm^2 and 4 μm apart, showing the extracted ΔI_E. The characteristics of a pair of PureB diodes of the same geometry with a 4 nm B-layer are shown for comparison.

In region (i), the series resistance is clearly responsible for the large attenuation, which will be higher for $I_{E//C}$ than for I_E, because the high collector current then also contributes to the voltage drop across the substrate. There are, however, also two hole-spreading effects that contribute to lowering $I_{E//C}$ with respect to I_E. The one is the difference in hole spreading into the substrate mentioned above and documented in [10]. Since the electron current is decades higher than the hole current, this small current difference is of no significance for ΔI_E. In contrast, the spreading of holes from one diode junction to the next has an enormous impact. In Fig. 5d, it is indicated that the few holes arriving at the neighboring diode will decrease the hole current across that junction. Accordingly, the electron current decreases to maintain the electron-to-hole ratio governed by the effective Gummel numbers of the n- and p-type regions. Thus, a very small change in hole current can induce a noteworthy decrease in $I_{E//C}$. In turn, this lowering of $I_{E//C}$ also reduces the effect of series resistance. Thus, as the voltage is decreased, the influence of series resistance on $I_{E//C}$ is decreased. Hence n is decreasing in the region (ii), and finally, a point can be reached where the influence of series resistance is so small that $I_{E//C}$ becomes larger than I_E, whereby ΔI_E becomes negative.

III. Experimental 2-Diode Results

The diode arrays discussed in Section II.A and pictured in Fig. 2a were used to investigate whether the 2-diode method could help in deciding whether or not abnormally high diode currents originate from an entire p-region that is Schottky-like, or from a small, localized nano-Schottky on an otherwise p$^+$n-like diode surface. In particular, we consider the possibility that the position of a nano-Schottky on the emitter surface will influence ΔI_E, i.e., the closer the nano-Schottky is to the collector, the greater will be the concentration of holes

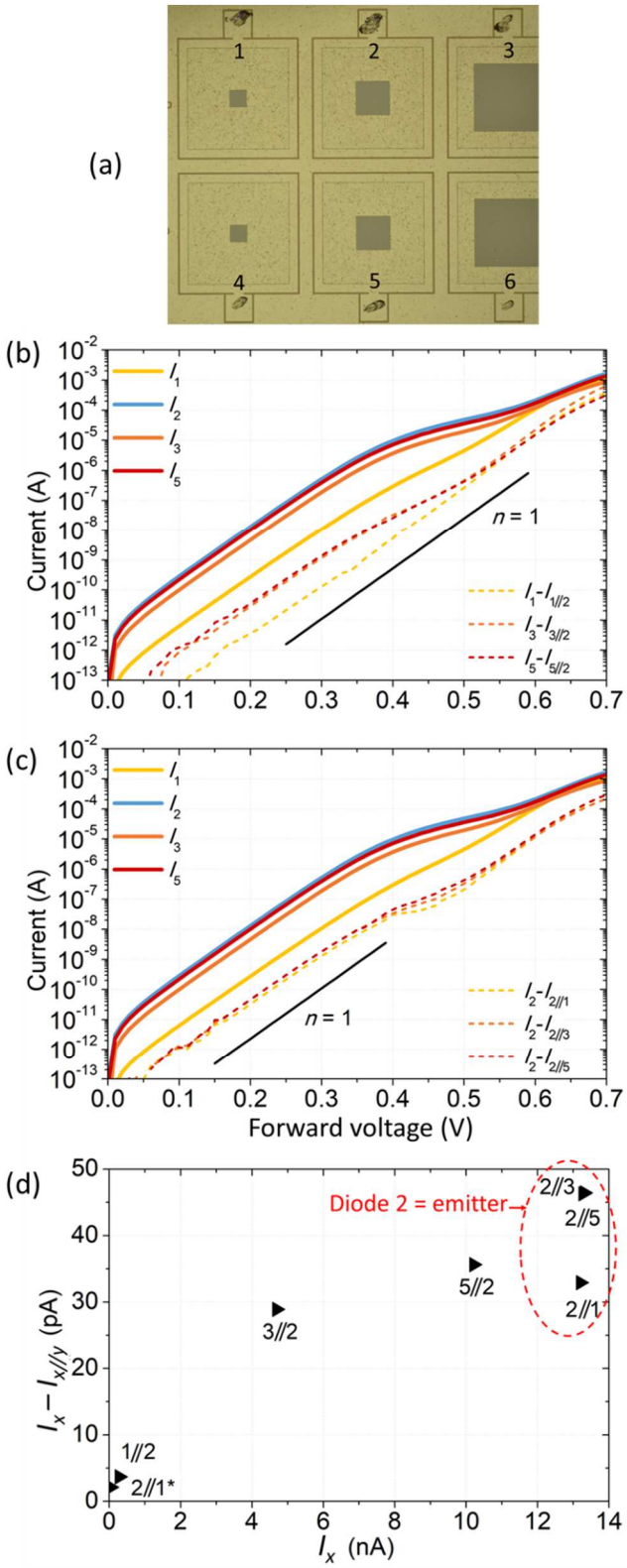

Fig. 8. (a) Micro-image of a set of 6 300×300 μm^2 diodes and their numbering as used in the measurement of (b) the 2-diode *I-V* characteristics and the extracted $\Delta I_{x//y}$ of diodes 1, 3, or 5 as emitter with diode 2 as the collector, and (c) of diode 2 as emitter with diodes 1, 3, or 5 as collector. (d) The extracted $\Delta I_{x//y}$ measured at 0.2 V forward bias, as a function of the corresponding emitter diode current, I_x. The point marked with an asterisk (2//1*) was found for the diodes of Fig. 6.

spreading there, resulting in a larger reduction of $I_{E//C}$ than if the nano-Schottky was far away.

An example of 2-diode extraction for emitter and collector diodes that show ideal behavior was given in Fig. 6. All *I-V* curves have $n = 1$ until they are attenuated by the series resistance. A set of 6 diodes as shown in Fig. 8a was selected for the nano-Schottky study. The diodes 1, 2, 3, and 5 were measured in different configurations and the nomenclature $\Delta I_{x//y}$ is used for the extracted differential current with diode x as emitter and diode y as collector. In Fig. 8b, each of the diodes 1, 3, and 5 was used as emitter with diode 2 as collector. Diode 1 has a barely noticeable excess current and kink, and the resulting $\Delta I_{1//2}$ curve is almost identical to the ΔI_E found for the ideal diodes of Fig. 6. For diodes 3 and 5 which have very noticeable kinks, the $\Delta I_{3//2}$ and $\Delta I_{5//2}$ display a kink that follows the magnitude of the emitter kink. The large excess current seen in diode 2 does not play a role, which is understandable since only the spreading of the holes from collector diode 2 to the emitter diodes causes a reduction in emitter current.

In Fig. 8c, diode 2 with the largest kink plays the role of emitter and the resulting *I-V* characteristics are shown for diodes 1, 3, or 5 as collector. In this case, the magnitude of the kink for the 3 different $\Delta I_{2//y}$ does not follow the emitter kink so clearly. This is made more evident in Fig. 8d, where the $\Delta I_{x//y}$ current at 0.2 V forward bias is plotted as a function of the corresponding emitter current.

Bipolar Gummel plots with biasing as shown in Fig. 5b were also considered. If bipolar transistors are available with the diode-under-test (DUT) as emitter, high current gain, close to ideal base current, and no punch-through at low voltages, the base current will be considerably lowered and any nano-Schottky current would be more visible. This would normally require vertical BJT's but more often only lateral BJT's can be fabricated. For these, the base current is more or less equal to the emitter current and does not add any useful information as illustrated by the example of Fig. 9.

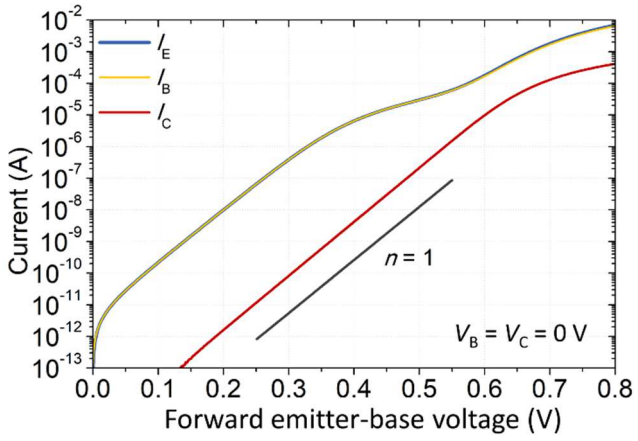

Fig. 9. Bipolar Gummel plot of a lateral BJT with diode 2 as emitter and diode 3 as collector.

IV. 2-DIODE TEST STRUCTURE OPTIMIZATION

Based on the results in Section III, it seems plausible that in a sufficiently large diode, the position of any nano-Schottky with respect to the collector diode will influence the level of the electron current contributing to the differential current. To mitigate effects that reduce the chances of getting an ideal differential current in a wide enough voltage region, we propose designs like the ones illustrated in Fig. 10 for achieving a position-dependent measurement.

In the design, we assume that the emitter diode is so large that the influence of a nano-Schottky near the edge is significantly different from one in the central region. At the moment, we do not have enough experimental evidence to determine what that size should be, but current spreading into the substrate, for a substrate resistivity of 2-5 ohm-cm, would be in the order of a few hundred microns. Therefore, sizes of 100 µm or more should be suitable. For higher substrate doping, i.e., shorter diffusion lengths, smaller sizes may be suitable.

Several other aspects have been considered:

- If the emitter and substrate series resistance are low enough, ideal ($n = 1$) differential currents can be extracted. To minimize the influence of series resistance in general, the current levels should be kept as low as possible.
- The current levels in the collector diodes should be minimized by using small widths. In this way, the hole spreading near the emitter remains high, but the electron current, which is proportional to the diode area, is minimized. Therefore, the influence on the substrate series resistance is minimized and even at relatively high nano-Schottky currents, the current spreading from the collector to the emitter may dominate the differential current.
- If possible, the collector regions should be made with high Gummel number p^+ regions with a low probability of nano-Schottky formation. This would also lower the electron current in the collector and reduce series resistance effects.
- The collectors and emitter should be placed close to each other to increase the flow of hole current from the collectors to the emitter as much as possible. In the test structures of Fig. 8a used here, the distance is an extremely large 96 µm and thus far from optimal.

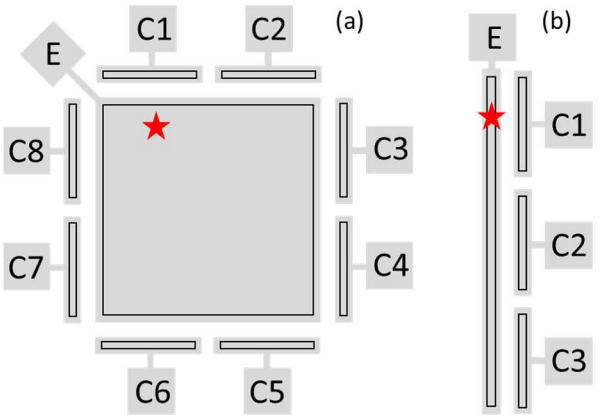

Fig. 10. Proposed test structure designs for 2-diode measurements where several collectors are placed around the perimeter of the emitter, (a) for a large area emitter and (b) for a long narrow emitter. For example, for a nano-Schottky at the position of the red star, collector C1 would induce a larger increase in ΔI_E than the other collectors.

In cases where the diode currents are so high that the series resistance attenuates the curve over the entire forward biasing region, it would still be possible to use test structures such as those in Fig. 10 to determine whether or not a local defect is a source of high current. This is because, although the $\Delta I_{x//y}$ has far from ideal behavior as discussed in Section III, it would still depend strongly on the hole spreading from the collector to the position on the emitter with the excess electron current.

V. Conclusions

In many of the experiments reviewed here, the signature of a nano-Schottky in the diode *I-V* measurements was the appearance of 2 regions with each $n \approx 1$, the one being a high-current region at low forward voltages that was connected by a kink at about 0.5 V to a region with ideally low current levels. Statistical data collection of such *I-V* characteristics was a reliable way of identifying random nano-Schottky distributions. Complementing with temperature-dependent measurements proved to be a powerful means to study the kink behavior and confirm the Schottky-like properties in individual cases. Arrays of diodes with a variety of sizes and perimeter-to-area ratios were also instrumental in identifying the presence of localized high-current defects.

The present results demonstrate that the differential *I-V* characteristics extracted from 2-diode measurements can also be a useful tool in discerning whether excess currents originate from Schottky-like contacts or from localized defects behaving as nano-Schottky diodes. A 2-diode design strategy was developed by which it would be possible to gain information on the location of nano-Schottky defects on large diode surfaces. This method potentially offers the advantage of being insensitive to parasitic effects such as non-ideal *g-r* currents and series-resistance current attenuation, which can completely obscure the kink behavior.

Acknowledgment

This work was supported by the B-Power Project No. 17979 of The Netherlands Organization for Scientific Research (NWO) Domain Applied and Engineering Sciences (TTW, and the Croatian Science Foundation under the project IP-2018-01-5296.

References

[1] L. K. Nanver L. Qi, V. Mohammadi, K. R. M. Mok, W. B. de Boer, N. Golshani, A. Sammak, T. L. M. Scholtes, A. Gottwald, U. Kroth, and F. Scholze, "Robust UV/VUV/EUV PureB photodiode detector technology with high CMOS compatibility," IEEE J. Sel. Topics Quantum Electron., vol. 20, no. 6, pp. 306–316, Nov. 2014, doi:10.1109/JSTQE.2014.2319582.

[2] L. Qi, K.R.C. Mok, M. Aminian, E. Charbon, and L.K. Nanver, "UV-sensitive low dark-count PureB single-photon avalanche diode," IEEE Transactions on Electron Devices, vol. 61, no. 11, pp. 3768-3774, Nov. 2014. doi: 10.1109/TED.2014.2351576.

[3] A. Sakic, G. van Veen, K. Kooijman, P. Vogelsang, T. L. M. Scholtes, W. de Boer, W. H. A. Wien, S. Milosavljevic, and L. K. Nanver, "High-efficiency silicon photodiode detector for sub-keV electron microscopy," *IEEE Trans. Electron Devices*, vol. 59, no. 10, pp. 2707–2714, Oct. 2012. doi: 10.1109/TED.2012.2207960.

[4] Lin Qi, S. Sluyterman, K. Kooijman, K. R. C. Mok, and Lis K. Nanver, "PureB single-photon avalanche diodes for low-energy electron detection down to 200 eV," Opt. Lett. 40, 300-303, 2015. doi.org/10.1364/OL.40.000300.

[5] B. Wang, R. Jia, K. Tao, W. Luo, L. Wang, D. Zhang, J. Chen, C. Lin, Y. Yang, X. Li, X. Ouyang, "The high energy resolution of Pt/Si alpha particle detector with Al2O3 passivation layer," Materials Science in Semiconductor Processing, vol. 152, 107054, 2022. https://doi.org/10.1016/j.mssp.2022.107054.

[6] N. Bhardwaj, B.B. Upadhyay, B. Parvez, P. Pohekar, Y. Yadav, A. Sahu, M. Patil, S. Basak, J. Sahu, and F.S.A. Sabiha, "Improved RF-DC characteristics and reduced gate leakage in GaN MOS-HEMTs using thermally grown Nb_2O_5 gate dielectric," 2023 Phys. Scr., vol. 98, p. 015805, 2023. doi: 10.1088/1402-4896/aca438

[7] T. Hashizumea, K. Nishiguchia, S. Kanekia, J. Kuzmikb, and Z. Yatabec, "State of the art on gate insulation and surface passivation for GaN-based power HEMTs," Materials Science in Semiconductor Processing, vol. 78, pp. 85-95, May 2018. https://doi.org/10.1016/j.mssp.2017.09.028

[8] J.T. Asubar, Z. Yatabe, D. Gregusova, and T. Hashizume, "Controlling surface/interface states in GaN based transistors: Surface model, insulated gate, and surface passivation," J. Appl. Phys., vol. 129, p. 121102, Mar. 2021. https://doi.org/10.1063/5.0039564

[9] M. Labed, J. Young Min, J.Y. Hong, Y.-K. Jung, S. Kyoung, K.W. Kim, K. Heo, H. Kim, K. Choi, N. Sengouga, Y.S. Rim, "Interface engineering of β-Ga_2O_3 MOS-type Schottky barrier diode using an ultrathin HfO_2 interlayer," Surfaces and Interfaces, vol. 33, 102267, 2022. doi.org/10.1016/j.surfin.2022.102267.

[10] X. Liu, and L. K. Nanver "Comparing current flows in ultra shallow pn-/Schottky-like diodes with 2-diode test method," 2016 International Conference on Microelectronic Test Structures (ICMTS), pp. 190–195, 2016. doi:10.1109/ICMTS.2016.7476205

[11] J. van Zoeren, L.K. Nanver, "Checks on temperature during on-wafer I-V characterization of Si diodes made with 2-D interfacial layers," 2022 International Conference on Microelectronic Test Structures (ICMTS), pp.1-6, 2022. doi: 10.1109/ICMTS50340.2022.9898239.

[12] T. Knezevic, X. Liu, E. Hardeveld, T. Suligoj & L. K. Nanver, "Limits on thinning of boron layers with/without metal contacting in PureB Si (photo) diodes," IEEE Electron Device Lett., vol. 40, no. 6, pp. 858–861, Jun. 2019, doi: 10.1109/LED.2019.2910465.

[13] L. Qi & L. K. Nanver, "Sheet resistance measurement for process monitoring of 400 °C PureB deposition on Si," 2015 International Conference on Microelectronic Test Structures, pp. 169-174, 2015. doi: 10.1109/ICMTS.2015.7106135.

[14] T. Knežević, T. Suligoj, I. Capan & L.K. Nanver, "Low-Temperature Electrical Performance of PureB Photodiodes Revealing Al-Metallization-Related Degradation of Dark Currents," IEEE Transactions on Electron Devices, 68 (6), pp. 2810-281, 2021. doi:10.1109/TED.2021.3074117

[15] Tihomir Knežević, Lis K. Nanver, and Tomislav Suligoj "Minimization of dark counts in PureB SPADs for NUV/VUV/EUV light detection by employing a 2D TCAD-based simulation environment", Proc. SPIE 10912, Physics and Simulation of Optoelectronic Devices XXVII, 109120Y (26 February 2019); https://doi.org/10.1117/12.2508829

[16] M. Krakers, T. Knezevic, K.M. Batenburg, X. Liu, L.K. Nanver, "Diode design for studying material defect distributions with avalanche-mode light emission," 2020 International Conference on Microelectronic Test Structures (ICMTS), 9.2, pp. 1-4, April 6-9, 2020. doi: 10.1109/ICMTS48187.2020.9107933